Peptide-Induced Conformational Changes in the Molecular Chaperone DnaK†

Sergey V. Slepenkov and Stephan N. Witt*

Department of Biochemistry and Molecular Biology, Louisiana State University Medical Center, 1501 Kings Highway, Shreveport, Louisiana 71130-3932

Received July 20, 1998; Revised Manuscript Received September 30, 1998

ABSTRACT: DnaK, the 70 kDa molecular chaperone of *Escherichia coli*, adopts a high-affinity state in the presence of ADP that tightly binds its target peptide, whereas replacement of ADP by ATP induces a structural switch to a low-affinity chaperone state that weakly binds its target. An ∼15% decrease in tryptophan fluorescence of DnaK occurs in concert with this switch from the high- to low-affinity state. The reversibility of this structural transition in DnaK was investigated using rapid mixing and equilibrium fluorescence methods. The Cro peptide (MQERITLKDYAM) was used to mimic an unfolded substrate. When the Cro peptide is rapidly mixed with preformed low-affinity DnaK complexes (DnaK*−ATP), a rapid increase (k_{obs} = 3−30 s^{-1}) in the tryptophan fluorescence of DnaK occurs. We suggest that the Cro peptide induces the transition of the low-affinity state of DnaK back to the high-affinity state, without ATP hydrolysis. The combined results in this report are consistent with the minimal mechanism ATP + EP ⇔ ATP−EP ⇔ ATP−E* + P, where ATP binding (K_1) induces a conformational change and concerted peptide release (k_{off}), and peptide binding (k_{on}) to the low-affinity state (ATP−E*) induces the transition back to ATP−EP, a high-affinity state. At 25 °C, in the presence of the Cro peptide, values for K_1, k_{off}, and k_{on} are 22 μM, 3.3 s^{-1}, and 2.4 × 10^4 M^{-1} s^{-1}, respectively. Evidence for an equilibrium between closed and open forms of DnaK in the absence of ATP and peptide is also presented.

Members of the 70 kDa molecular chaperone family, composed of inducible (Hsp70) and constitutive (Hsc70) variants, mediate reactions such as the folding, assembly, and transport of proteins in the case of the constitutive 70 kDa chaperones and the renaturation of denatured proteins in the case of the inducible 70 kDa chaperones (for reviews, see refs *1*−*3*). In these different reactions, the molecular chaperone variants selectively bind to partially unfolded or disordered regions of other proteins in an activity cycle that is controlled by the binding and hydrolysis of ATP. The mechanism by which the binding and hydrolysis of ATP is coupled to the binding, retention, and release of polypeptides by these molecular chaperones is not known.

The architecture of 70 kDa molecular chaperones is defined by two distinct structural domains, the ∼44 kDa N-terminal domain which binds and hydrolyzes ATP (*4*) and the ∼23 kDa C-terminal domain which binds and releases polypeptide targets (*5*, *6*), whose activities are coupled in that ligand-induced conformational changes appear to be propagated from one domain to the other (*7*−*11*).

There is compelling evidence that shows that ATP binding rather than hydrolysis induces a conformational change in the ATPase domain that is propagated to the polypeptide-binding domain, resulting in a reduced affinity of polypeptide substrates for the C-terminal domain of DnaK, the 70 kDa chaperone expressed by *Escherichia coli* (*8*, *9*). In concert with the ATP-induced transition, an ∼15% reduction in the tryptophan fluorescence of the chaperone occurs together with a blue shift of the fluorescence spectrum (*12*, *13*). This ATP-induced conformational transition in DnaK has been referred to as the high-to-low-affinity transition (*8*). Conversely, since polypeptide binding stimulates the rate of chaperone-catalyzed hydrolysis of ATP (*7*, *14*, *15*), polypeptide binding must affect the conformation of the ATPase domain. However, direct evidence for a peptide-induced conformational change in DnaK has been difficult to obtain.

The thrust of this report is that specific peptide binding to the low-affinity state of DnaK in vitro triggers a rapid increase (k_{obs} = 3−30 s^{-1}) in tryptophan fluorescence. This peptide-induced increase in fluorescence is unrelated to ATP hydrolysis, because k_{cat} equals 6.7 × 10^{-3} s^{-1} under the conditions of these experiments (*16*). The results are consistent with a peptide-induced conformational change in DnaK; peptide binding to the low-affinity state triggers a rapid, concerted return to the high-affinity state.

MATERIALS AND METHODS

Protein and Reagents. All reagents were of the highest purity and were purchased from Sigma, unless stated otherwise. DnaK was isolated as previously described (*16*) and stored at 4 °C in the sample buffer [25 mM *N*-(2-hydroxyethyl)piperazine-*N*′-2-ethanesulfonic acid/50 mM KCl/5 mM $MgCl_2$/5 mM 2-mercaptoethanol (pH 7.0)]. Additional details on the preparation of DnaK can be found in a previous paper (*17*) which showed that after exhaustive dialysis DnaK preparations were assayed for endogenous nucleotide; 94% of the DnaK molecules were nucleotide-free.

† Support for this work came from the NIH (GM51521) and an American Cancer Society Junior Faculty Research Award (JFRA-583).

* To whom correspondence should be addressed. Telephone: (318) 675-7891. Fax: (318) 675-5180. E-mail: switt1@ lsumc.edu.

10.1021/bi981738k CCC: $15.00
Published on Web 11/06/1998

Peptides were purchased from the University of Kentucky Macromolecular Core Facility. The Cro[1] peptide (MQERITLKDYAM) was used because of its known ability to bind to DnaK (*18*), whereas the poly-L-glutamic acid (Sigma) and the VSV5 peptide (LFRPK) were used as nonbinding controls; the VSV13 peptide (KLIGVLSSLFRPK), which also binds to DnaK (*19*), was also used in some experiments. The peptides purchased from the University of Kentucky Macromolecular Core Facility were purified on a C_4 reversed phase column (Vydac, model 214TP1010) using a water/acetonitrile gradient. The Cro peptide was specifically labeled at its N terminus with dansyl chloride as described previously (*16*). The dansyl-Cro peptide, fCro, was purified on a C_4 reversed phase column (Vydac, model 214TP1010) using a water/acetonitrile gradient. Unlabeled peptides were sequenced to verify identity, whereas the mass of the fCro conjucate was verified by electrospray mass spectrometry (Louisiana State University Core Facility, New Orleans, LA). The average molecular mass of the control peptide, poly-L-glutamic acid, was 1 kDa; this compound was used without additional purification.

Instrumentation. Rapid kinetic measurements were taken with an Applied Photophysics Ltd. (Leatherhead, U.K.) stopped-flow fluorescence spectrometer (SX-18MV), which has a 1.5 ms dead time. The dimensions of the optical cell where mixing and detection occur equaled 1 cm × 0.2 cm × 0.1 cm. Excitation occurred through the 0.2 cm path and detection through the 0.1 cm path. The conditions under which the different types of rapid kinetic experiments were conducted are described below.

ATP-Induced Decrease in the Tryptophan Fluorescence of DnaK. (i) For the experiments where no peptide was used, ATP (2−2000 μM) was contained in one syringe, while DnaK (2 μM) was contained in the other. Traces from these experiments followed double-exponential kinetics. (ii) For the experiments where the Cro peptide was used, preformed DnaK−Cro complexes were prepared by preincubating DnaK with Cro for ∼2 h at room temperature. Preformed complexes were contained in one syringe, and ATP was contained in the other syringe. Two variations of these experiments were conducted. In one set of experiments, the concentration of the preformed DnaK−Cro complexes was fixed and the concentration of ATP was varied; in the other set of experiments, DnaK at a fixed concentration was preincubated with the Cro peptide at increasing concentrations and then the solution mixed with ATP at a fixed concentration. The traces from both these experiments followed single-exponential kinetics. For experiments i and ii, the excitation wavelength was 295 nm (1.5 or 2.5 nm bandwidth), and stray excitation radiation was eliminated with either a 320 or 335 nm Oriel long-pass filter. Last, experiments were conducted with 295 nm excitation to minimize the possibility of artifacts due to an inner filter effect from ATP. Note that the absorbance at 295 nm of a 1 mM solution of ATP (A_{295} = 0.015) is negligible when the path length equals 1 cm. Moreover, since the path length of our stopped-flow cell is 0.2 cm, there is no appreciable inner filter effect at high ATP concentrations.

ATP-Induced Dissociation of fCro from Preformed DnaK−fCro Complexes. The dissociation of fCro from preformed DnaK−fCro complexes was probed as follows. ATP (1 mM) and unlabeled Cro (40 μM) were contained in one syringe, and DnaK (4 μM) and fCro (1 μM) were contained in the other. The latter solution was allowed to preincubate for 2 h at the desired temperature so it could form DnaK−fCro complexes. When the solutions were mixed, there was a decrease in dansyl fluorescence due to the dissociation of bound fCro. The dissociation traces followed single-exponential kinetics. The excitation wavelength was 335 nm (2.5 nm bandwidth), and stray excitation radiation was eliminated with a 399 nm Oriel long-pass filter.

Cro Peptide-Induced Increase in the Tryptophan Fluorescence of DnaK. The effect of Cro peptide binding to the low-affinity state of DnaK was probed as follows. The low-affinity state of DnaK, represented as ATP−E*, was prepared by mixing DnaK (2 μM) with excess ATP (2 mM). One syringe was loaded with the solution of low-affinity complexes and the other with varying amounts of the Cro peptide (40−800 μM). The Cro peptide-induced increase in the tryptophan fluorescence of DnaK followed single-exponential kinetics. The excitation wavelength was 295 nm (1.5 or 2.5 nm bandwidth), and stray excitation radiation was eliminated with either a 320 or 335 nm Oriel long-pass filter.

In all stopped-flow experiments, the instrumental time constant was equal to 0.5% of the half-time of the fastest phase. All stopped-flow traces are the average of four to ten individual traces. In some cases, data were collected using a split time base mode. Temperature control of both the jacketed reactants and the jacketed mixing chamber was achieved with a circulating external water bath ($\Delta T = \pm 0.2$ °C). The concentrations in the text refer to those after mixing.

Steady state fluorescence measurements were made with a Photon Technology Inc. (South Brunswick, NJ) StrobeMaster lifetime spectrometer with a SE-900 steady state fluorescence option that utilizes a 75 W xenon arc lamp as an excitation source with photon counting detection (PTI model 710). Fluorescence spectra with a λ_{ex} of 295 (4 nm band-pass) were recorded ∼100 s after the addition of ATP to samples of DnaK and peptide. Samples were maintained in a quartz cuvette (1 cm path length) which was stirred constantly, and temperature control was achieved via an external circulating heating and cooling bath ($\Delta T = \pm 0.2$ °C). The sample temperature was verified using a hand-held thermocouple which was placed directly into the sample.

Curve Fitting and Simulations. Stopped-flow data were fitted to single- or double-exponential functions using a curve fitting program that used a Marquardt algorithm based on the program Curfit described by Bevington (*20*). Kinetic mechanisms were simulated using the program KINSIM (*21*), and the simulated progress curves were fitted to single- and double-exponential functions using KaleidaGraph (Synergy Software, Reading, PA). Eyring plots were analyzed and standard errors determined also using KaleidaGraph. The error associated with the reported rates, rate constants, and amplitudes varies between 10 and 20%.

[1] Abbreviations: Cro, synthetic peptide representing residues 1−12 of the cro repressor protein (MQERITLKDYAM); fCro, α-amino dansyl-Cro peptide; VSV5, synthetic peptide representing residues 498−502 of the vesicular stomatitis virus glycoprotein expressed by the New Jersey serotype of the virus (LFRPK); VSV13, synthetic peptide representing residues 490−502 of the vesicular stomatitis virus glycoprotein expressed by the New Jersey serotype of the virus (KLIGVLSSLFRPK).

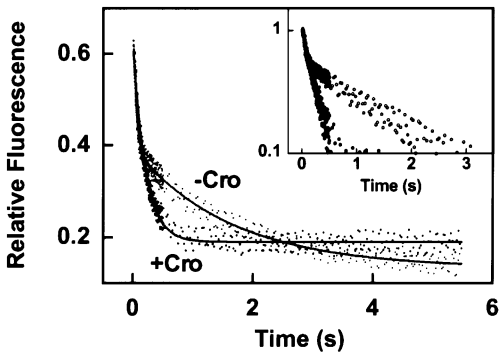

FIGURE 1: Effect of Cro peptide on the kinetics of the ATP-induced decrease in tryptophan fluorescence of DnaK. Mixing preformed DnaK−Cro complexes with ATP yielded a single-exponential decrease in fluorescence, $F(t) = 0.42 \exp(-4.7\ s^{-1} \times t) - 0.41$ (solid line). In contrast, mixing DnaK only with ATP yielded a double-exponential decrease in fluorescence, $F(t) = 0.28 \exp(-18.1\ s^{-1} \times t) + 0.26 \exp(-0.61\ s^{-1} \times t) - 0.49$ (solid line). In the inset are shown plots of log $[F(t) - F_\infty]/(F_o - F_\infty)$ vs time. Concentrations after mixing were 1.3 μM DnaK, 0 or 25 μM Cro, and 500 μM ATP; the temperature was 25 °C.

RESULTS

Effect of Bound Cro Peptide on ATP-Induced Spectral Changes in DnaK. We reported previously that in the absence of peptide ATP induces a biphasic reduction in the tryptophan fluorescence of DnaK (*17*), and that the reduction in fluorescence occurs before ATP hydrolysis. For example, when DnaK was rapidly mixed with 500 μM ATP at 25 °C (Figure 1), the decrease in fluorescence followed double-exponential kinetics, $F(t) = \Delta F_1 e^{-1/\tau_1} + \Delta F_2 e^{-t/\tau_2} + F_\infty$, with the fast and slow rates, $1/\tau_1$ and $1/\tau_2$, being equal to 18.1 and 0.61 s^{-1}, respectively, and the amplitudes, ΔF_1 and ΔF_2, being equal to 0.28 and 0.26, respectively. Interestingly, when DnaK was preincubated for 2 h with the Cro peptide ([Cro]/[DnaK] = 40)[2] and then rapidly mixed with ATP (Figure 1), the decrease in fluorescence followed single-exponential kinetics, $F(t) = \Delta F e^{-t/\tau_{ATP}} + F_\infty$, with $1/\tau_{ATP}$ and ΔF being equal to 4.7 s^{-1} and 0.42, respectively. The inset compares semilog plots of the two traces. An explanation of how a DnaK-bound peptide affects the kinetics of ATP binding is given in the Discussion.

Rapid Kinetics of ATP Binding to Preformed DnaK−Cro Complexes. To understand the mechanism of the coupling between the ATPase domain and the peptide binding domain of DnaK, the reaction between ATP and preformed DnaK−peptide complexes (ATP + EP) was probed over a range of temperatures (15−35 °C) and ATP concentrations using stopped-flow fluorescence. Preformed DnaK−peptide complexes were prepared using the Cro peptide, which mimics an unfolded polypeptide substrate (*16*). The rapid mixing of ATP with a nearly homogeneous population of preformed DnaK−Cro complexes resulted in a single-exponential decrease in the tryptophan fluorescence of DnaK at 25 °C (Figures 1 and 2A), with the rate of the decrease being equal to $1/\tau_{ATP}$. Single-exponential kinetics were also obtained at 15 and 35 °C (data not shown). Plots of the rates versus ATP concentration are hyperbolic (Figure 2B). The asymptotes of the plots, $(1/\tau_{ATP})_{max}$, are 0.86, 3.4, and 13.4 s^{-1} at 15, 25, and 35 °C, respectively (Table 1).

[2] Cro dissociates from DnaK with a K_d of approximately 6 μM (*16*).

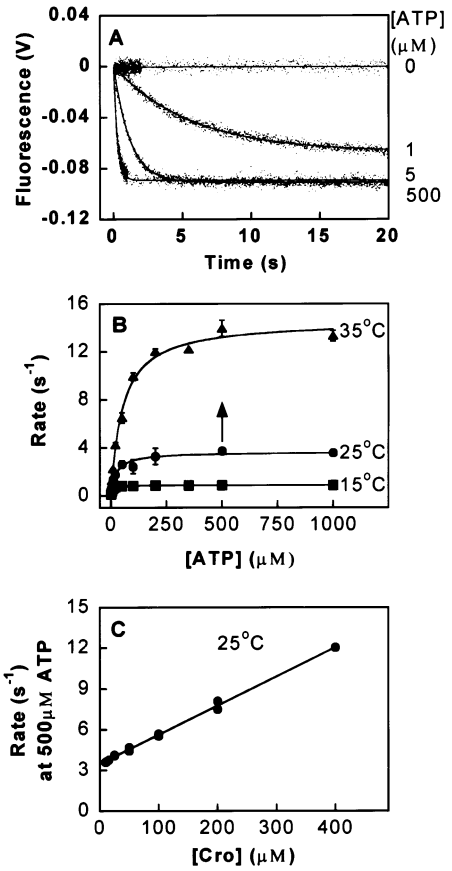

FIGURE 2: (A) Kinetics of the ATP-induced decrease in the tryptophan fluorescence of DnaK−Cro peptide complexes monitored by stopped-flow fluorescence. Traces follow the relationship $F(t) = \Delta F e^{-t/\tau_{ATP}} + F_\infty$ (solid lines), with rates, $1/\tau_{ATP}$, equal to 0.18, 0.80, and 3.6 s^{-1} at 1, 5, or 500 μM ATP, respectively. Final concentrations after mixing were 1.0 μM DnaK and 20 μM Cro; the temperature was 25 °C. V is volts. (B) Plots of the rate ($1/\tau_{ATP}$) vs [ATP] at constant Cro concentration. Data points are the average of two or three determinations conducted on different days. Data are fit to $1/\tau_{ATP} = k_{on}[P] + k_{off}[ATP]/(K_1 + [ATP])$ (solid lines). The asymptote of each plot equals $k_{on}[P] + k_{off}$. The vertical arrow above the point at 500 μM ATP (25 °C) indicates that the asymptote increases with increasing concentrations of Cro peptide. (C) Plot of the rate of fluorescence decrease ($1/\tau_{ATP}$) (●) vs [Cro] at a constant ATP concentration (500 μM). Rates were determined by preincubating DnaK with increasing concentrations of the Cro peptide and then mixing with excess ATP. The slope and *y*-intercept are k_{on} [$(2.1 \pm 0.1) \times 10^4\ M^{-1}\ s^{-1}$] and k_{off} ($3.5 \pm 0.1\ s^{-1}$), respectively. Final concentraions after mixing were 1 μM DnaK, 10−400 μM Cro, and 500 μM ATP; the temperature was 25 °C.

The minimal mechanism consistent with these above results is the two-step mechanism depicted in Scheme 1. The first step is rapid ATP binding that produces a ternary complex between ATP, DnaK, and peptide (ATP−EP). The second step is a conformational switch; bound ATP triggers the forward conformational change (k_{off}) and the concerted release of the bound peptide (P), and concomitant with the conformational change is a reduction in the tryptophan fluorescence of DnaK (denoted by the asterisk). Conversely, peptide binding induces the reverse conformational change (k_{on}), which occurs with an increase in tryptophan fluorescence (see below). EP and ATP−EP are high-affinity states, whereas ATP−E* is the low-affinity state. More elaborate mechanisms are described in the Appendix.

For Scheme 1, when ATP and peptide are in excess over DnaK and a rapid equilibrium is assumed for the bimolecular

Table 1: Kinetic and Thermodynamic Constants for the Reactions of DnaK Species with ATP and Peptide

	ATP-induced decrease in DnaK−peptide complex fluorescence[a]		ATP-induced peptide dissociation[b]	peptide-induced increase in DnaK*−ATP complex fluorescence[c]	
temperature (°C)	$(1/\tau_{ATP})_{max}$ (s^{-1})	K_1 (μM)	k_{off} (s^{-1})	k_{off} (s^{-1})	k_{on} (M^{-1} s^{-1})
15	0.86 ± 0.03	5 ± 1	0.78 ± 0.02	0.68 ± 0.02	(9.9 ± 0.7) × 10^3
25	3.4 ± 0.5	22 ± 8	3.3 ± 0.1	2.9 ± 0.5	(2.4 ± 0.4) × 10^4
35	13.4 ± 0.7	52 ± 6	11.1 ± 0.4	11.9 ± 1.0	(5.2 ± 0.3) × 10^4

[a] $(1/\tau_{ATP})_{max}$ is the asymptote of the plots in Figure 2B. K_1 values were determined from the fit of each plot to $1/\tau_{ATP} = k_{on}[Cro] + k_{off}[ATP]/K_1 + [ATP]$. [b] k_{off} determined from single-exponential fits of the data in Figure 3. [c] k_{off} and k_{on} are the *y*-intercept and slope, respectively, of the plots in Figure 5D. The $(1/\tau_{ATP})_{max}$ parameter can be used to calculate k_{off}. Given that $(1/\tau_{ATP})_{max} = k_{on}[P] + k_{off}$, and [P] = 20 μM, calculated values for k_{off} are 0.66 ± 0.03, 2.9 ± 0.5, and 12.4 ± 0.6 s^{-1} at 15, 25, and 35 °C, respectively.

Scheme 1

$$\mathrm{ATP} + \mathrm{EP} \underset{}{\overset{K_1}{\Leftrightarrow}} \mathrm{ATP\text{-}EP} \overset{k_{off}}{\underset{k_{on}}{\Leftrightarrow}} \mathrm{ATP\text{-}E^*} + \mathrm{P}$$

reaction ATP + EP ⇔ ATP−EP, the rate of the ATP-induced decrease in the tryptophan fluorescence of DnaK in terms of the equilibrium constant K_1 and rate constants k_{off} and k_{on} is described by

$$1/\tau_{ATP} = k_{on}[P] + \frac{k_{off}[ATP]}{K_1 + [ATP]} \quad (1)$$

A plot of $1/\tau_{ATP}$ versus [ATP] is hyperbolic, and when [ATP] ≫ K_1, the asymptote, $(1/\tau_{ATP})_{max}$, is given by

$$(1/\tau_{ATP})_{max} = k_{on}[P] + k_{off} \quad (2)$$

To verify eq 2, experiments were conducted to determine whether the asymptote of the plots in Figure 2B depends on the Cro peptide concentration. Specifically, DnaK was preincubated with increasing concentrations of the Cro peptide and then rapidly mixed with a large excess of ATP at 25 °C. Figure 2C shows that the asymptote, that is, the rate at 500 μM ATP, increased linearly with increasing Cro peptide concentrations. The slope and *y*-intercept of the plot are k_{on} [(2.1 ± 0.1) × 10^4 M^{-1} s^{-1}] and k_{off} (3.5 ± 0.1 s^{-1}), respectively. This linear dependence of the asymptote of the plot in Figure 2B on Cro peptide concentration strongly supports Scheme 1.

Given the above values for k_{on} and k_{off}, and because the Cro peptide concentration was only 20 μM in the kinetic experiments, we reasonably conclude that the asymptote of the plots in Figure 2B slightly overestimates the first-order rate constant k_{off}. For example, at 25 °C, $k_{on}[P]$ = 2.1 × 10^4 M^{-1} s^{-1} × 20 × 10^{-6} M = 0.42 s^{-1}, whereas k_{off} = 3.5 s^{-1}. The $(1/\tau_{ATP})_{max}$ parameter overestimates k_{off} by 10−15%.

Kinetics of fCro Peptide Dissociation from Preformed DnaK−fCro Complexes. The effect of ATP on the dissociation of the Cro peptide from DnaK was probed using an N-terminally dansylated version of the Cro peptide (fCro). When excess ATP was mixed with preformed DnaK−fCro complexes, a single-exponential decrease in the signal occurred, consistent with the dissociation of the bound fCro peptide (Figure 3). The magnitudes of these apparent off-rate constants are similar to the magnitudes of the asymptotes in Figure 2B (Table 1), consistent with Scheme 1.

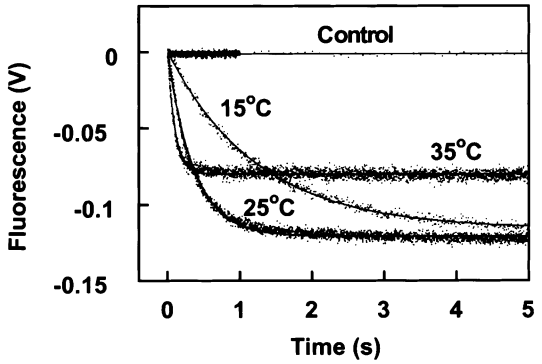

FIGURE 3: Kinetics of fCro dissociation from preformed DnaK−fCro complexes monitored by stopped-flow fluorescence. Dissociation traces follow the relationship $F(t) = \Delta F e^{-k_{off}t} + F_\infty$ (solid lines), with k_{off} being equal to 0.80, 3.1, and 11.5 s^{-1} at 15, 25, and 35 °C, respectively. Final concentrations after mixing were ∼1 μM DnaK−fCro, 1 mM ATP, and 30 μM Cro. In control experiments, DnaK−fCro complexes were mixed with buffer.

Effect of the Cro Peptide on the Tryptophan Fluorescence of Low-Affinity DnaK−ATP Complexes. According to Scheme 1, specific peptide binding should inhibit the ability of ATP to reduce the tryptophan fluorescence of DnaK. To test this idea, ATP was added to DnaK pre-equilibrated with varying amounts of the Cro peptide, and the subsequent reduction in tryptophan fluorescence was assessed. For example, when DnaK was preincubated with a large excess of the Cro peptide, the addition of 1 or 500 μM ATP either had no effect or induced a 2% reduction in tryptophan fluorescence, respectively (Figure 4A). On the other hand, when DnaK was preincubated with a large excess of either VSV5 or poly-L-glutamic acid, which are nonbinding controls, the addition of 1 or 500 μM ATP induced a 15% reduction in tryptophan fluorescence (Figure 4A). The results, summarized in Figure 4B, reveal that specific Cro peptide binding inhibits the ATP-induced reduction in the tryptophan fluorescence of DnaK.

Rapid Kinetics of Cro Peptide Binding to Preformed Low-Affinity DnaK Complexes. The reaction between the Cro peptide and preformed low-affinity DnaK−ATP complexes (P + ATP−E*), a reversal of the second step of Scheme 1, was examined using stopped-flow fluorescence. A rapid increase in tryptophan fluorescence occurred when excess Cro peptide (400 μM) was rapidly mixed with preformed low-affinity DnaK complexes (Figure 5A, top trace). In contrast, a rapid decrease in tryptophan fluorescence occurred when excess ATP (500 μM) was rapidly mixed with preformed DnaK−Cro complexes (Figure 5A, bottom trace). Note that the change in signal induced by the Cro peptide is equal in magnitude but opposite in sign with respect to the change in signal induced by ATP. As a control, excess Cro

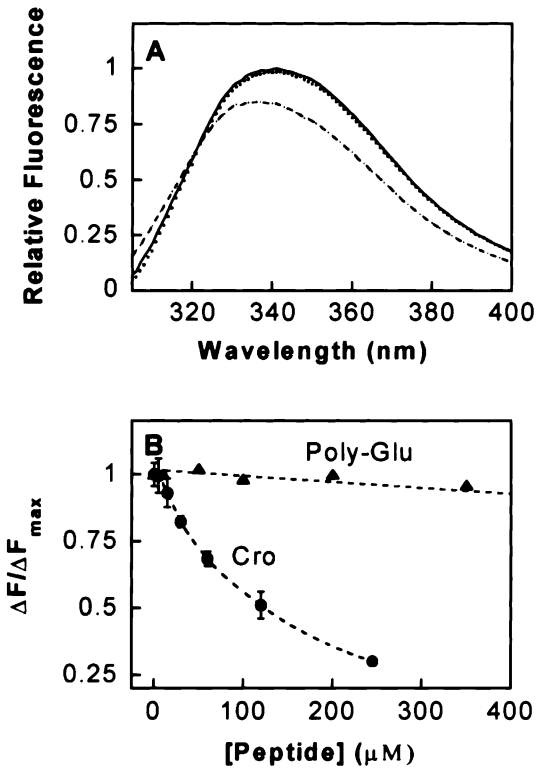

FIGURE 4: (A) Steady state fluorescence spectra of DnaK: DnaK and Cro (—); DnaK and Cro, followed by the addition of ATP (···); and DnaK with either no peptide or a nonbinding control peptide (VSV5), followed by the addition of ATP (—·—). Final concentrations were 1 μM DnaK, 400 μM peptide, and 500 μM ATP. (B) Plot of $\Delta F/\Delta F_{max}$ vs [peptide]. ΔF_{max} is the maximum change in fluorescence, which occurs in the absence of polypeptide or with the control peptides (LFRPK or polyglutamic acid). Dashed lines are to guide the eye.

peptide (400 μM) was mixed with DnaK; no spectral change occurred in this control (Figure 5A, middle trace). These results demonstrate that the Cro peptide induces a rapid increase in the fluorescence of the low-affinity DnaK complexes. Such results are consistent with a peptide-induced transition from the low-affinity state to the high-affinity state.

The reaction between the Cro peptide and preformed low-affinity DnaK−ATP complexes was also probed by conducting mixing experiments where the concentration of preformed low-affinity complexes was fixed and the concentration of Cro peptide was varied. Traces from such experiments are shown in Figure 5B. Each trace followed single-exponential kinetics, $F(t) = \Delta F(1 - e^{-t/\tau_{Cro}}) + F_o$, where $1/\tau_{ATP}$, ΔF, and F_o are the rate, amplitude, and initial fluorescence, respectively. The amplitudes increase to a maximum value (Figure 5C), and the rates exhibit a linear increase with increasing concentrations of the Cro peptide (Figure 5D). Both of these results are consistent with the reaction P + ATP−E* ⇔ ATP−EP. In addition, the slope and *y*-intercept of the rate versus [Cro] plots are k_{on} and k_{off} (Table 1), respectively. The k_{off} values, ranging from 0.68 to 11.9 s^{-1} between 15 and 35 °C, are nearly identical to the k_{off} values obtained from the direct dissociation experiments and to the asymptotes of the plots of $1/\tau_{ATP}$ versus ATP concentration (see Table 1).

The temperature dependence of k_{off} was also determined (Table 1). Eyring plots (data not shown) of k_{off} determined from (i) the ATP-induced decrease in the fluorescence of DnaK−P complexes (Figure 2B), (ii) the off-rate kinetic experiments (Figure 3), and (iii) the Cro peptide-induced increase in the fluorescence of low-affinity DnaK-ATP complexes (Figure 5D) could be superimposed with an activation enthalpy (ΔH^*) and entropy (ΔS^*) equal to 23 ± 1 kcal mol^{-1} and 22 ± 5 cal mol^{-1} K^{-1}, respectively.

Several experiments were also conducted using the VSV13 peptide (data not shown). The preincubation of DnaK with 40 μM VSV13 followed by the rapid mixing with ATP also resulted in a single-exponential decrease in the fluorescence of DnaK; fVSV13 dissociated from preformed DnaK−fVSV13 complexes upon mixing with ATP with an apparent first-order rate constant ($k_{off} = 7.1 \pm 0.9$ s^{-1}) that was almost identical to the maximal rate of ATP-induced decrease in the tryptophan fluorescence of DnaK−VSV13 complexes, and the preincubation of DnaK with excess VSV13 inhibited the ability of ATP to reduce the fluorescence of DnaK.

DISCUSSION

Effect of Bound Peptide on the Kinetics of ATP-Induced Spectral Changes in DnaK. An intriguing observation in this report was that ATP binds to DnaK molecules devoid of bound peptide with double-exponential kinetics, whereas ATP binds to DnaK−peptide complexes with single-exponential kinetics (Figure 1). This phenomenon can be explained if the ATPase domain of DnaK equilibrates between closed and open forms, and the equilibrium is affected by the presence of peptide. Such an equilibrium is reasonable since the ATPase domain of hexokinase, which is a structural homologue of the ATPase domain of 70 kDa chaperones (*4*), equilibrates between closed and open forms (*22*). Therefore, suppose that the ATPase domain of DnaK equilibrates between closed and open states in the absence of peptide according to

$$ {}_{c}E \underset{k_{oc}}{\overset{k_{co}}{\rightleftharpoons}} {}_{o}E \qquad (3) $$

where E represents the DnaK monomer and the subscripts c and o indicate that the mouth of the ATPase domain is closed and open, respectively. We propose that in the absence of peptide, ATP binds to the open and not the closed conformation of DnaK according to

$$ {}_{c}E \underset{k_{oc}}{\overset{k_{co}}{\rightleftharpoons}} {}_{o}E + ATP \underset{k_{-1}}{\overset{k_{1}}{\rightleftharpoons}} ATP-{}_{o}E \underset{k_{-2}}{\overset{k_{2}}{\rightleftharpoons}} ATP-E^* \qquad (4) $$

where the asterisk indicates a state with reduced tryptophan fluorescence relative to that of the E state.

Reaction 4 was simulated to test whether the simulated traces were biphasic. Biphasic simulated traces are obtained when $k_{co} = k_{oc} = 0.7$ s^{-1}, $k_1 = 10^5$ M^{-1} s^{-1}, $k_{-1} = 1$ s^{-1}, $k_2 = 20$ s^{-1}, and $k_{-2} = 0.1$ s^{-1} and $[{}_{c}E] = [{}_{o}E] = 0.5$ μM and $[ATP-{}_{o}E] = [ATP-E^*] = 0$ at time zero; the values for the fluorescence factors are as follows: $F({}_{c}E) = F({}_{o}E) = F(ATP-{}_{o}E) = 1.0$ and $F(ATP-E^*) = 0.85$. In fact, biphasic simulated traces are obtained as long as $k_{co} \approx k_{oc}$ and $k_2 + k_{-2} \gg k_{co} + k_{oc}$. Simulated traces were fit to a double-exponential function using KaliedaGraph. Plots of the calculated rates versus ATP concentration are shown in Figure 6. The asymptotes of the plots of the fast and slow

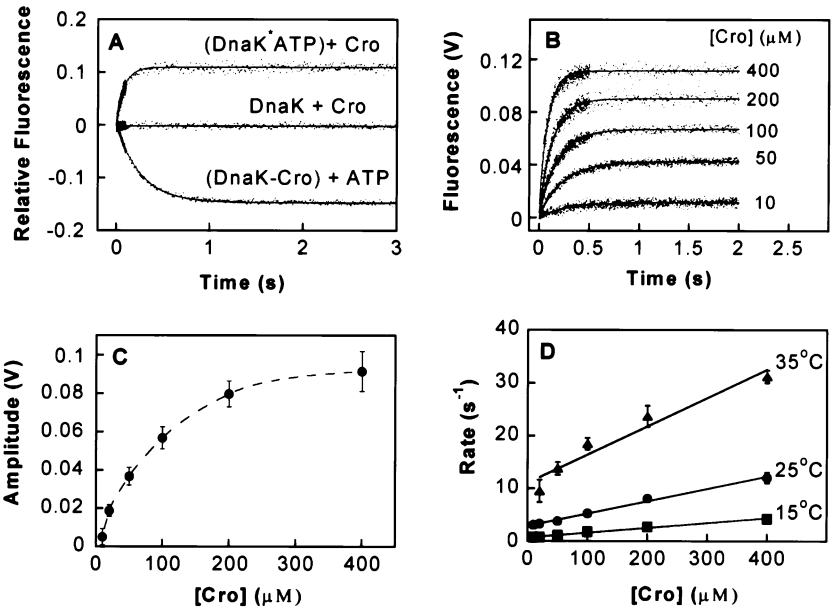

FIGURE 5: (A) Comparison of the changes in the tryptophan fluorescence of DnaK due to three reactions: (i) Cro and low-affinity DnaK complexes (top trace), (ii) Cro and DnaK (middle trace), and (iii) ATP and DnaK−Cro complexes (bottom trace). Final concentrations after mixing were (i) 1 μM DnaK, 400 μM Cro, and 500 μM ATP, (ii) 1 μM DnaK and 400 μM Cro, and (iii) 1 μM DnaK, 20 μM Cro, and 500 μM ATP. (B) Kinetics of Cro peptide-induced increase in the tryptophan fluorescence of low-affinity DnaK complexes (Cro + ATP-E*). Traces follow the relationship $F(t) = \Delta F(1 - e^{-t/\tau_{Cro}}) + F_o$ (solid line), with rates $1/\tau_{Cro}$ being equal to 3.3, 4.2, 5.4, 7.5, and 11.5 s^{-1} at 10, 50, 100, 200, and 400 μM Cro, respectively. The temperature was 25 °C; the ATP concentration was 500 μM. (C) Plot of the amplitude ΔF vs [Cro]. The dashed line is to guide the eye. (D) Plots of the rate ($1/\tau_{Cro}$) of Cro-induced increase in the tryptophan fluorescence of DnaK vs [Cro]. Data were fit to the equation $1/\tau_{Cro} = k_{on}[Cro] + k_{off}$ (solid lines). Values for k_{on} and k_{off} are listed in Table 1.

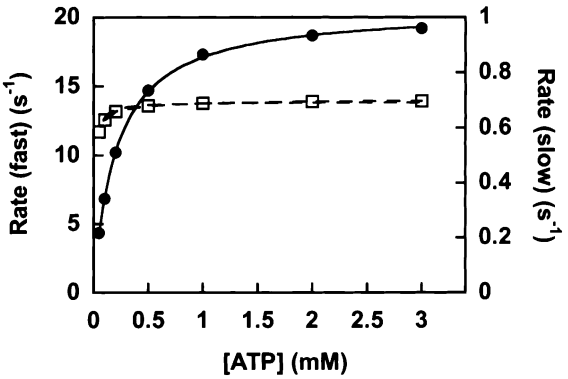

FIGURE 6: Plot of calculated rates of the ATP-induced decrease in the tryptophan fluorescence of DnaK vs [ATP]. Calculated rates were determined from the simulation of reaction 4 with the following parameters and initial conditions: $k_{co} = k_{oc} = 0.7$ s^{-1}, $k_1 = 10^5$ M^{-1} s^{-1}, $k_{-1} = 1$ s^{-1}, $k_2 = 20$ s^{-1}, and $k_{-2} = 0.1$ s^{-1} and $[_cE] = [_oE] = 0.5$ μM at time zero; and fluorescence factors $F(_cE) = F(_oE) = F(ATP-{}_oE) = 1.0$ and $F(ATP-{}_oE^*) = 0.85$. The simulated traces followed double-exponential kinetics: (●) fast rate and (□) slow rate.

rate are 20 and 0.7 s^{-1}, respectively. This indicates that the rapid phase of fluorescence decrease according to reaction 4 is due to the ATP−$_o$E → ATP−E* transition, and the slow phase of fluorescence decrease is due to the $_c$E → $_o$E transition. On the basis of this simulation, we conclude that reaction 4 can explain the biphasic ATP-induced spectral changes in DnaK that occur in the absence of peptide (Figure 1).

Suppose that specific peptide binding shifts the population of chaperone molecules to the $_o$E state according to

$$_cE \Leftrightarrow {}_oE + P \rightarrow {}_oEP \qquad (5)$$

ATP then binds to the $_o$EP complexes by the two-step reaction

$$ATP + {}_oEP \overset{K_1}{\leftrightarrow} ATP-{}_oEP \underset{k_{on}}{\overset{k_{off}}{\leftrightarrow}} ATP-E^* + P \qquad (6)$$

where a rapid bimolecular reaction occurs in the first step and a conformational change with concerted peptide release and a reduction in fluorescence occur in the second step. With these steps, the ATP-induced decrease in fluorescence follows single-exponential kinetics. Reaction 6 is equivalent to Scheme 1. Reactions 3−6 reasonably explain the ATP-induced spectral changes in DnaK that occur in both the presence and absence of peptide.

To summarize, the following results support Scheme 1, or reaction 6. (i) The values for k_{off}, determined from three different experiments, are nearly identical (Table 1). (ii) The asymptote of the plot of $1/\tau_{ATP}$ versus Cro peptide concentration is determined by the relationship $k_{on}[Cro] + k_{off}$ (Figure 2C). (iii) Two different types of mixing experiments gave the same values for k_{on}. The plot of $1/\tau_{ATP}$ versus Cro peptide concentration yielded a k_{on} of $(2.1 \pm 0.1) \times 10^4$ M^{-1} s^{-1} at 25 °C, and the plot of $1/\tau_{Cro}$ versus Cro peptide concentration yielded a k_{on} of $(2.4 \pm 0.4) \times 10^4$ M^{-1} s^{-1} (compare Figure 2C to Figure 5D). (iv) Cro peptide binding rather than Cro peptide-stimulated ATP hydrolysis causes the low-to-high-affinity switch in the structure of DnaK, because the rate of DnaK-catalyzed ATP hydrolysis is 6.7×10^{-3} s^{-1} (37 °C, 400 μM Cro) (*16*), while the rate of the Cro-induced increase in the tryptophan fluorescence of DnaK is 32 s^{-1} (35 °C, 400 μM Cro) (Figure 5D). (v) Our results are also consistent with the VSV13 peptide reacting according to Scheme 1.

Cro Peptide Binding to the Low-Affinity State of DnaK (P + ATP−E ⇔ ATP−EP).* Values for k_{on} and k_{off} for the reaction between the Cro peptide and preformed low-affinity

DnaK complexes were determined. An attempt was made to verify these values by monitoring the change in fluorescence due to fCro peptide binding to preformed low-affinity complexes. Unfortunately, the fluorescence signal was so weak that reproducible data could not be obtained. On the other hand, the k_{off} values obtained from the direct dissociation experiments (Figure 3) are almost identical to the values obtained from the experiments where Cro peptide was mixed with preformed low-affinity DnaK complexes (see Table 1).

Peptide Association (P + ATP−E → ATP−EP).* It is interesting to examine the effect of ATP on the magnitude of k_{on}. In the absence of ATP, fCro binds to DnaK, which is a state presumed to be equivalent to a high-affinity state of DnaK, with k_{on} values ranging from 8 to 200 M^{-1} s^{-1} between 15 and 35 °C (*16*). Over the same temperature range, the Cro peptide binds to DnaK in the presence of excess ATP with k_{on} values ranging from 9900 to 52 000 M^{-1} s^{-1}. The presence of ATP therefore accelerates the rate of Cro peptide binding to DnaK by a factor of 1240−260, depending on the temperature. The effect of ATP on the activation enthalpy (ΔH^*) barrier to Cro peptide binding is also significant; for fCro peptide binding to DnaK in the absence of ATP, $\Delta H^* = 26 \pm 8$ kcal mol^{-1} (*16*), whereas for Cro peptide binding to DnaK in the presence of ATP, $\Delta H^* = 15 \pm 1$ kcal mol^{-1} (Table 1). If it is assumed that the polypeptide binding site is closed in the high-affinity state and open in the low-affinity state, the $\Delta(\Delta H^*)$ value of 11 kcal mol^{-1} is the amount of heat needed to open the closed polypeptide binding site in the absence of ATP.

Peptide Dissociation (EfP + ATP → ATP−E + fP).* At 25 °C, fCro dissociates from preformed DnaK−fCro complexes with a k_{off} of 3.3 s^{-1} in the presence of ATP. In contrast, at the same temperature, fCro dissociates from preformed DnaK−fCro complexes with a k_{off} of 1.2×10^{-4} s^{-1} in the absence of ATP (*16*). Thus, ATP accelerates the release of fCro from DnaK by a factor of 25 000. We have shown that ATP induces a high-to-low-affinity state conformational transition in a DnaK−peptide complex that results in the concerted dissociation of the bound peptide and suggest that the same conformational transition must occur even in the absence of ATP for a bound peptide to dissociate from a DnaK−peptide complex. This means that the value 1.2×10^{-4} s^{-1} is probably the first-order rate constant for the uncatalyzed high-to-low-affinity conformational transition in a DnaK−peptide molecular complex and that the large ΔH^* value of 34 ± 1 kcal mol^{-1}, determined for the dissociation of fCro from preformed DnaK−fCro complexes in the absence of ATP (*16*), is probably the activation enthalpy for this uncatalyzed high-to-low-affinity conformational transition in DnaK. The activation enthalpy for the ATP-catalyzed high-to-low-affinity conformational transition in DnaK is 23 ± 1 kcal mol^{-1}. If it is assumed that the lid of the polypeptide binding domain closes over the bound peptide in the high-affinity state (*6*), the heat, $\Delta(\Delta H^*)$, required to open the closed polypeptide binding site in the absence of ATP is 11 kcal mol^{-1}. This $\Delta(\Delta H^*)$ value is identical to the $\Delta(\Delta H^*)$ value determined from the association experiments (see above).

Comparison to Previous Studies. Compare our k_{on} (2.4×10^4 M^{-1} s^{-1}) and k_{off} (3.3 s^{-1}) values at 25 °C for the reaction between the Cro peptide and preformed low-affinity complexes to the results from other studies. Schmid and co-workers (*9*) found that in the presence of ATP the 21-mer targeting signal pre-piece of the precursor of mitochondrial aspartate aminotransferase (pp-1) binds to DnaK with k_{on} and k_{off} being equal to 4.5×10^5 M^{-1} s^{-1} and 1.8 s^{-1}, respectively. Theyssen and co-workers (*13*) found that in the presence of ATP a 24-mer synthetic peptide dissociates from DnaK with a k_{off} of 3.8 s^{-1}. On the basis of Scheme 1, we predict that the sequence of the peptide dictates the magnitude of k_{on}, whereas the rate of the ATP-induced conformational change in a DnaK−peptide complex primarily dictates the rate of peptide release. Thus, for the reaction between peptide and preformed low-affinity DnaK complexes, considerable variation is expected in the magnitude of k_{on} but much less variation in the magnitude of k_{off}. The limited available data agree with this idea.

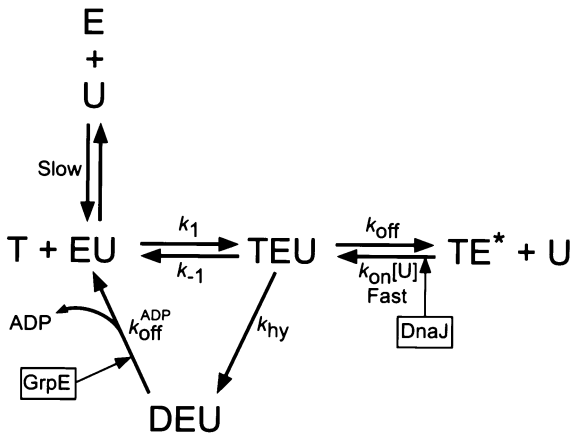

FIGURE 7: Proposed reaction cycle of DnaK in vivo.

Proposed in Vivo Reaction Cycle of DnaK. Molecular chaperones with masses of 70 kDa have cochaperones that function to modulate their activity in vivo. For example, in *E. coli*, the cochaperones DnaJ and GrpE modulate the activity of DnaK (*23*, *24*). A model is presented in Figure 7 that indicates how DnaJ and GrpE might promote or accelerate certain steps in the DnaK activity cycle. It is likely that in vivo, like in vitro, an unfolded polypeptide molecule, U, binds to the low-affinity state, ATP−E*, with a relatively large rate but with low affinity ($K_d \sim 150$ μM). DnaJ probably plays a pivotal role in vivo by serving to increase the affinity of U for the chaperone low-affinity state either by directly "presenting" U to an ATP−E* molecule (*25*), which increases the local concentration of unfolded polypeptide, or by binding to a ATP−E* molecule in such a way that the activation energy barrier to the low-to-high-affinity switch is lowered. Hydrolysis of ATP occurs from the ATP−EU state, generating the ADP−EU state. Nucleotide exchange, catalyzed or uncatalyzed depending on the organism, is followed by ATP binding, which switches the chaperone molecule back to the low-affinity state.

ACKNOWLEDGMENT

We thank Drs. Robert Rhoads and Arthur Veis for their critical reading of the manuscript.

APPENDIX

Consider two alternative mechanisms for ATP binding to DnaK−peptide complexes. First, consider the three-step sequential reaction

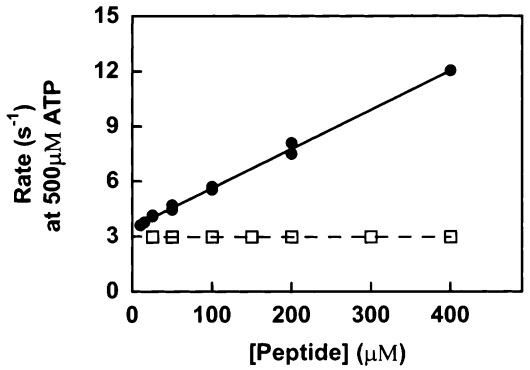

FIGURE 8: Plot of the calculated rate of the ATP-induced decrease in tryptophan fluorescence of DnaK−peptide complexes vs peptide concentration. Calculated rates (□) were determined from the simulation of reaction 7 with the following parameters and initial conditions: $K_1 = 22\ \mu M$, $k_2 = 3\ s^{-1}$, $k_{-2} = 0.1\ s^{-1}$, $k_3 = 0.1$ or 30 s^{-1}, and $k_{-3} = 2 \times 10^4\ M^{-1}\ s^{-1}$; initial concentrations of 1 μM EP, 20−400 μM peptide, and 500 μM ATP and [ATP−EP] = [ATP−E*P] = [ATP−E*] = 0 at time zero; fluorescence factors F(EP) = F(ATP−EP) = 1 and F(ATP−E*P) = F(ATP−E*) = 0.85. Simulated traces followed single-exponential kinetics. For comparison, the observed rate (●) of the ATP-induced decrease in the fluorescence of DnaK vs Cro peptide concentration is also plotted (see Figure 2C).

$$\mathrm{ATP} + \mathrm{EP} \overset{K_1}{\Leftrightarrow} \mathrm{ATP{-}EP} \underset{k_{-2}}{\overset{k_2}{\Leftrightarrow}} \mathrm{ATP{-}E^*P} \underset{k_{-3}}{\overset{k_3}{\Leftrightarrow}} \mathrm{ATP{-}E^*} + \mathrm{P} \quad (7)$$

where ATP binding, a conformational change, and peptide release occur sequentially, and the asterisk denotes a state with reduced fluorescence relative to that of the EP state. Such a reaction, where peptide release is coupled to the second step of ATP binding but the dissociation of peptide is rate-limiting ($k_3 < k_2$), was suggested by Theyssen and co-workers (*13*). Reaction 7 was simulated to determine the effect of peptide on the rate of the ATP-induced reduction in fluorescence of the chaperone molecules with the following initial conditions and parameters: $K_1 = 22\ \mu M$, $k_2 = 3\ s^{-1}$, $k_{-2} = 0.1\ s^{-1}$, $k_3 = 0.1$ or 30 s^{-1}, and $k_{-3} = 2 \times 10^4\ M^{-1}\ s^{-1}$; initial concentrations of 1 μM EP, 20−400 μM peptide, and 500 μM ATP; and fluorescence factors F(EP) = F(ATP−EP) = 1 and F(ATP−E*P) = F(ATP−E*) = 0.85. Simulated traces followed single-exponential kinetics. The simulations revealed that the rate ($1/\tau_{ATP}$) of the ATP-induced decrease in the fluorescence of the chaperone molecules at a constant ATP concentration (500 μM) does not depend on the concentration of peptide (Figure 8). For comparison, the plot of the rate of ATP-induced reduction in the tryptophan fluorescence of DnaK versus Cro peptide concentration (Figure 2C) is superimposed on the plot in Figure 8. On the basis of this comparison, we conclude that reaction 7 cannot explain the results in this report.

Second, consider the three-step sequential reaction

$$\mathrm{ATP} + \mathrm{EP} \overset{K_1}{\Leftrightarrow} \mathrm{ATP{-}EP} \underset{k_{-2}}{\overset{k_2}{\Leftrightarrow}} \mathrm{ATP{-}E} + \mathrm{P} \underset{k_{-3}}{\overset{k_3}{\Leftrightarrow}} \mathrm{ATP{-}E^*} \quad (8)$$

In this reaction, ATP binding to the molecular chaperone−peptide complex yields a ternary complex (ATP−EP) in the first step; ternary complex formation triggers a conformational change that releases the bound peptide in the second step, and in the third step, peptide release triggers a second conformational change that results in the formation of the low-affinity state (ATP−E*), which has reduced fluorescence relative to that of the EP state. Peptide binding to the low-affinity state induces the switch back to a high-affinity state according to the reaction ATP−E* + P ⇔ ATP−E′P. This latter species has the same intrinsic fluorescence as ATP−EP but a different conformation. This mechanism cannot be ruled out.

REFERENCES

1. Georgopoulos, C., and Welch, W. J. (1993) *Annu. Rev. Cell Biol. 9*, 601−634.
2. Hendrick, J. P., and Hartl, F.-U. (1993) *Annu. Rev. Biochem. 62*, 349−384.
3. Becker, G., and Craig, E. A. (1994) *Eur. J. Biochem. 219*, 11−23.
4. Flaherty, K. M., DeLuca-Flaherty, C., and McKay, D. B. (1990) *Nature 346*, 623−628.
5. Morshauser, R. C., Wang, H., Glynn, G. C., and Zuiderweg, R. P. (1995) *Biochemistry 34*, 6261−6266.
6. Zhu, X., Zhao, X., Burkholder, W. F., Gragerov, A., Ogata, C. M., Gottesman, M. E., and Hendrickson, W. A. (1996) *Science 272*, 1606−1614.
7. Flynn, G. C., Chappell, T. G., and Rothman, J. E. (1989) *Science 245*, 385−390.
8. Palleros, D. R., Reid, K. L., Shi, L., Welch, W. J., and Fink, A. L. (1993) *Nature 365*, 664−666.
9. Schmid, D., Baici, A., Gehring, H., and Christen, P. (1994) *Science 263*, 971−973.
10. Buchberger, A., Theyssen, H., Schroder, H., McCarty, J. S., Virgallita, G., Milkereit, P., Reinstein, J., and Bukau, B. (1995) *J. Biol. Chem. 270*, 16903−16910.
11. Fung, K. L., Hilgenberg, L., Wang, N. M., and Chirico, W. J. (1996) *J. Biol. Chem. 271*, 21559−21565.
12. Palleros, D. R., Reid, K. L., McCarty, J. S., Walker, G. C., and Fink, A. L. (1992) *J. Biol. Chem. 267*, 5279−5285.
13. Theyssen, H., Schuster, H.-P., Packschies, L., Bukau, B., and Reinstein, J. (1996) *J. Mol. Biol. 263*, 657−670.
14. Sadis, S., and Hightower, L. E. (1992) *Biochemistry 31*, 9406−9412.
15. Blond-Elguindi, S., Fourie, A. M., Sambrook, J. F., and Gething, M.-J. H. (1993) *J. Biol. Chem. 268*, 12730−12735.
16. Farr, C. D., Galiano, F. J., and Witt, S. N. (1995) *Biochemistry 34*, 15574−15582.
17. Slepenkov, S. V., and Witt, S. N. (1998) *Biochemistry 37*, 1015−1024.
18. Gragerov, A., Zeng, L., Zhao, X., Burkholder, W., and Gottesman, M. E. (1994) *J. Mol. Biol. 235*, 848−854.
19. Buchberger, A., Valencia, A., McMacken, R., Sander, C., and Bukau, B. (1994) *EMBO J. 13*, 1687−1695.
20. Bevington, P. R. (1969) *Data Reduction and Error Analysis for the Physical Sciences*, pp 92−96, McGraw-Hill, New York.
21. Barshop, B. A., Wrenn, R. F., and Frieden, C. (1983) *Anal. Biochem. 130*, 134−145.
22. Anderson, C. M., Stenkamp, R. E., McDonald, R. C., and Steitz, T. A. (1978) *J. Mol. Biol. 123*, 207−219.
23. Szabo, A., Langer, T., Schroder, H., Flanagan, J., Bukau, B., and Hartl, F.-U. (1994) *Proc. Natl. Acad. Sci. U.S.A. 91*, 10345−10349.
24. Hartl, F. U. (1996) *Nature 381*, 571−580.
25. Jordan, R., and McMacken, R. (1995) *J. Biol. Chem. 270*, 4563−4569.

BI981738K